

# Ethylacetate extract from *Tetrastigma hemsleyanum* induces apoptosis via the mitochondrial caspase-dependent intrinsic pathway in HepG<sub>2</sub> cells

Xin Peng<sup>1</sup> · Yuan-yuan Zhang<sup>2</sup> · Jin Wang<sup>3</sup> · Qingyong Ji<sup>1</sup>

Received: 21 April 2015 / Accepted: 15 May 2015 / Published online: 9 August 2015  
© International Society of Oncology and BioMarkers (ISOBM) 2015

**Abstract** Ethylacetate extract of *Tetrastigma hemsleyanum* (EET) has a potent antitumor activity in vitro and in vivo. However, the molecular mechanism underlying EET-induced apoptosis remains elusive. As part of our continuing studies, we investigated the apoptosis mechanism of HepG<sub>2</sub> cells exposed to different concentrations of EET in vitro. Confocal laser scanning was used to detect the apoptotic morphological changes. Flow cytometer and inverted fluorescence microscope were used to detect the mitochondrial membrane potential and cytosolic Ca<sup>2+</sup> level. Western blotting analysis was used to evaluate the expression of the apoptosis-related proteins. Annexin V/PI staining was used to investigate cell apoptosis. Spectrophotometry was used to detect the activity of caspase family. The results showed that distinct apoptotic morphological changes occurred in HepG<sub>2</sub> cells treated by EET. EET caused collapse of mitochondrial membrane potential, elevation of cytosolic Ca<sup>2+</sup> level, and evoked release of cytochrome c from mitochondria in a concentration-dependent manner. The apoptosis was accompanied by a significant activation of caspase-3, caspase-9, and the cleavage of

poly (ADP-ribose) polymerase, but there was no significant change in either the activity or the expression level of caspase-8. Furthermore, EET-induced apoptosis could be inhibited by caspase-9 inhibitor Z-LEHD-FMK but not by caspase-8 inhibitor Z-IETD-FMK. Taken together, these overall results demonstrated that EET-induced apoptosis of HepG<sub>2</sub> cells was mediated by the mitochondrial caspase-dependent intrinsic pathway rather than the death receptor/caspase-8-mediated signaling route.

**Keywords** *Tetrastigma hemsleyanum* · HepG<sub>2</sub> cells · Apoptosis · Caspase · Ca<sup>2+</sup>

## Introduction

Hepatocellular carcinoma (HCC), the most common type of malignancies worldwide, is the fourth leading cause of cancer-related deaths in the world [1]. The major treatment methods are surgery, chemotherapy, and radiotherapy; however, the effect is not satisfactory. There is an urgent need to identify novel therapeutic agents for the treatment of HCC. The failure to control cancer cell death associated with the induction of apoptosis has been considered to be a critical cause of resistance against cancer therapy [2]. Nowadays, the use of apoptosis-inducing agents from herbal prescriptions has gained a great deal of interest for the treatment of cancer. These plant extracts have been explored for discovering potential natural therapeutic compounds due to their excellent pharmacological activities and low side effects [3].

*Tetrastigma hemsleyanum* Diels et Gilg is a rare and endangered medicinal plant native to China. This plant is traditionally used as alternative herbal medicine for the treatment of hepatitis and rheumatic arthritis and regulating immune function [4]. Previous findings have demonstrated that the

✉ Xin Peng  
px4142@163.com; pengx@mail.zjpc.net.cn

Yuan-yuan Zhang  
cpuzhang27@163.com

Jin Wang  
975091745@qq.com

Qingyong Ji  
sanyeqing@126.com

<sup>1</sup> Institute of Biopharmaceutical, Zhejiang Pharmaceutical College, Ningbo 315100, Zhejiang, China

<sup>2</sup> Nanjing General Hospital of Nanjing Military Command, Nanjing 210095, China

<sup>3</sup> Nanjing Agriculture University, Nanjing 210095, China

lipid soluble substances extracted from *T. hemsleyanum* exhibited strong cytotoxicity towards a variety of cancers, such as leukemia and carcinomas of the lung and intestine [5]. In vivo study has also shown that the ethylacetate extract of *T. hemsleyanum* has antitumor and immunomodulatory activities in H22 liver of tumor-bearing mice [6]. Our previous study also showed that ethylacetate extract of *T. hemsleyanum* (EET) inhibited cell growth through arresting the cell cycle, and the protein expression of Bax and P53 was increased while that of Bcl<sub>2</sub> was significantly decreased [7]. Therefore, we hypothesized that EET-induced HepG<sub>2</sub> cells toxicity might also involve cell apoptosis, but the molecular mechanism of cell apoptosis induced by EET remained poorly understood.

To date, researches indicate that apoptotic signals may proceed through two main pathways, intrinsic (mitochondrial) related to cytochrome c release into the cytosol and extrinsic associated with the activation of death receptors [8]. Indeed, many anticancer agents used in clinical therapy intervene with apoptotic signaling, either with the intrinsic or the extrinsic pathway [9, 10].

To apply natural products to the cancer prevention or therapy, it is essential to elucidate their possible underlying molecular biological mechanism. Even though many researches had showed that EET could induce the apoptosis of various cancer cells, the exact link between apoptotic pathway and their activation has yet not been clarified. Therefore, the aim of the present study was to explore the potential molecular signaling pathways of EET-induced apoptosis in HepG<sub>2</sub> cells cultured in vitro. The role of mitochondrial membrane potential and caspases in this process were investigated; the effects of EET on apoptotic proteins in HepG<sub>2</sub> cells were also examined. These results were a basis for the later study on the anticancer mechanism and the medicinal value development of *T. hemsleyanum*.

## Materials and methods

### Antibodies and reagents

HepG<sub>2</sub> cells were purchased from Shanghai Institutes for Biological Sciences, Chinese Academy of Sciences; rabbit polyclonal antibodies against cytochrome c, caspase-8, caspase-3, caspase-9, and PRAP from Proteintech Group, USA; mouse monoclonal antibody against β-actin from Transgen Biotech, China; goat-anti-rabbit and goat-anti-mouse fluorescent markers-conjugated secondary antibodies from Licor, USA; BCA protein assay kit from Beyotime Biotech, China; Annexin V-FITC Apoptosis Detection Kit from Beyotime Biotech, China; mitochondrial membrane potential assay kit with JC-1 from (Beyotime Biotech, China; Caspase 3, Caspase 8, and Caspase 9 Activity Assay Kit from Beyotime Biotech, China; Cell Mitochondria Isolation Kit from

Beyotime Biotech, China; Z-LEHD-FMK and Z-IETD-FMK from Beyotime Biotech, China; fetal bovine serum from Sijiqing Biotech, China; RPMI1640 medium from (Invitrogen, USA; and Polyvinylidene fluoride membrane from (Millipore Life Science, USA.

### Preparation of EET

EET was prepared according to our previous study [7]. The powdered *T. hemsleyanum* root was refluxed with 95 % ethanol for three times, 1 h each time. Ethanol was removed and a splash of water was added to dissolve the remnant. Then, the solution was extracted with ethyl acetate, and the resulting extract was then vacuum dried. The dried extract was dissolved in dimethyl sulfoxide (DMSO) and the culture media, and the final concentration of DMSO was 0.1 % (v/v) and then filtered through a 0.22-μm micro-filtrate membrane.

### Cell culture

HepG<sub>2</sub> cells were cultured in RPMI 1640 (Invitrogen, USA), supplemented with 10 % fetal bovine serum (Sijiqing Biotech, China) and 50 U/ml penicillin–streptomycin (PAA, Pasching, Austria), and grown at 37 °C under saturated humidity with 5 % CO<sub>2</sub>.

### AO/EB double fluorescence staining

HepG<sub>2</sub> cells were seeded on the petri dishes at concentration of  $1 \times 10^6$  cells/ml and incubated overnight, then treated with EET (50, 100, and 200 μg/mL) or DMSO (0.1 %) for 24 h. The cells for fixation were washed twice with phosphate-buffered saline (PBS) and treated with 75 % ethanol for 2 h. After they were washed twice in PBS, HepG<sub>2</sub> cells were stained with 100 μg/mL acridine orange (AO) and 100 μg/mL ethidium bromide (EB) for 10 min. Confocal images were acquired with a confocal laser scanning microscope (Zeiss LSM 510, Germany). The fluorescence determination for AO was taken at Ex-488 nm and Em-520 nm and for EB was taken at Ex-543 nm and Em-590 nm.

### Apoptosis determination by Annexin V-FITC/PI staining

Cells were plated at  $5 \times 10^5$  cells/mL in six-well plates (Corning, USA) and incubated overnight; then, they were pretreated with caspase inhibitors (Z-LEHD-FMK or Z-IETD-FMK; 15 μM) or DMSO (vehicle) for 2 h and then exposed to EET (0–200 μg/mL) for 24 h. Cell apoptosis determination assays were conducted using an Annexin V-FITC Apoptosis Detection Kit following the manufacturer's instructions. Using flow cytometric analysis, scatterplot of cells with propidium iodide on the y-axis and annexin V on the x-axis, the percentages of both early and late apoptotic cells were

determined by a flow cytometer (BD FACSCalibur, USA). Data was analyzed using the CellQuest Pro software. A total of 10,000 events were counted, and three independent experiments were performed.

#### Assays of caspase-3, caspase-8, and caspase-9 activities

The detection of caspase-3, caspase-8, and caspase-9 activities were performed using the caspases activity assay kits following manufacturer's instructions. Briefly, HepG<sub>2</sub> cells were plated at  $5 \times 10^5$  cells/mL in six-well plates (Corning, USA) and incubated overnight, and then, they were exposed to EET (0–200  $\mu\text{g}/\text{mL}$ ) for different time periods. Cells were lysed and centrifuged for 20,000g for 15 min at 4 °C. The supernatants were normalized for protein content and incubated with the reaction buffer containing the corresponding substrates at 37 °C for 2 h. The optical density was quantified by spectrophotometric detection at 405 nm. The activities of caspase-3, caspase-8, and caspase-9 were expressed as mean percentage of control  $\pm$  SD from three experiments.

#### Western blotting

HepG<sub>2</sub> cells were seeded in six-well plates at concentration of  $1 \times 10^6$  cells/ml and treated with EET (50, 100, and 200  $\mu\text{g}/\text{mL}$ ) or DMSO (0.1 %) for 24 h. The total protein of the cells extracted with cell lysis buffer (20 mM Tris-HCl, pH 7.5, 150 mM NaCl, 0.5 % NP-40, 1 % Triton X-100, 1 mM PMSF) for 30 min at 4 °C. The lysates were clarified by centrifugation at 12,000g for 10 min at 4 °C. Supernatants were collected, and their protein concentrations determined using BCA protein assay kit. The lysates were boiled for 5 min at 100 °C. Fifty micrograms of protein extract was subjected to sodium dodecyl sulfate–polyacrylamide gel electrophoresis (SDS–PAGE) on 5 % attacking and 15 % resolving gel, then blotted onto a polyvinylidenedifluoride (PVDF) membrane, blocked with 5 % nonfat milk in TBS-Tween buffer (pH 7.5, 0.12 M Tris-base, 1.5 M NaCl, 0.1 % Tween20) for 1.5 h at room temperature, incubated with the corresponding primary antibodies separately overnight at 4 °C, and then incubated with fluorescent markers-conjugated secondary goat-anti-rabbit antibodies (1:5000 dilution, Licor, USA) or goat-anti-mouse (1:5000) at room temperature in the dark for 2 h. The blots were then analyzed for band densities using Odyssey CLX IR fluorescent scanning image systems (Licor, USA). The above primary antibodies were Rabbit polyclonal antibodies cytochrome c (1:500), caspase-8 (1:1000), caspase-3 (1:500), caspase-9 (1:500), PARP (1:500), and mouse monoclonal antibody  $\beta$ -actin (1:2000). Values were normalized to corresponding  $\beta$ -actin levels. The results were given as the mean  $\pm$  SD.

#### Determination of mitochondrial membrane potential

The disruption of mitochondrial membrane potential was detected using flow cytometer (BD FACSCalibur, USA) and inverted fluorescence microscope (Olympus bx51, Japan) equipped with a digital camera (magnification,  $\times 1000$ ). HepG<sub>2</sub> cells cultured in six-well plates were treated with EET (50, 100, and 200  $\mu\text{g}/\text{mL}$ ) or DMSO for 24 h, then they were harvested, washed twice, and resuspended in PBS. The assays were conducted using a mitochondrial membrane potential assay kit with JC-1 (5,5',6,6'-tetrachloro-1,1',3,3'-tetraethylbenzamidozolocarbocyanin iodide) (Beyotime Biotech, China), in accordance with the manufacturer's instructions. Stained cells were washed with PBS and immediately analyzed. The measurement for red fluorescence was taken at Ex-525 nm and Em-590 nm and for green fluorescence was taken at Ex-488 nm and Em-530 nm. The mitochondrial membrane potential is expressed as JC-1 fluorescence units in terms of red fluorescence to green fluorescence ratio. Three independent experiments were performed.

#### Detection of cytochrome c release

HepG<sub>2</sub> cells were seeded in six-well plates at concentration of  $1 \times 10^6$  cells/ml and treated with EET (50, 100, and 200  $\mu\text{g}/\text{mL}$ ) or DMSO for 24 h. Mitochondrial fractions were prepared using Cell Mitochondria Isolation Kit following manufacturer's instructions. Cells were harvested and washed with PBS twice and then incubated in mitochondrial separation reagent. The mixture was homogenated and centrifuged at 600g for 10 min; the supernatant was centrifuged at 10,000g for 15 min at 4 °C. The precipitate represented the mitochondrial fractions. The resultant supernatant was further centrifuged at 20,000g for 30 min at 4 °C to obtain cytosolic fractions. Equal amounts of protein were prepared for western blot studies. After SDS-PAGE in a 12 % gel, proteins were electrotransferred onto a PVDF membrane. The blots were incubated with anti-cytochrome c and were developed as described earlier.

#### Measurement of cytosolic $\text{Ca}^{2+}$ level

HepG<sub>2</sub> cells cultured in six-well plates were treated with EET (50, 100, and 200  $\mu\text{g}/\text{mL}$ ) or DMSO for 24 h, and then they were harvested, washed twice, and resuspended in D-Hank's buffer. Washed cells were loaded with 10  $\mu\text{M}$  Fluo-3/AM (Beijing Solarbio Biotech, China) containing 0.05 % Pluronic F<sub>127</sub> at 37 °C for 20 min, and then the cells were washed twice with 4-(2-hydroxyethyl)-1-piperazineethanesulfonic acid (HEPES) buffer saline (10 mM HEPES, 1 mM Na<sub>2</sub>HPO<sub>4</sub>, 137 mM NaCl, 1 mM CaCl<sub>2</sub>, 5 mM KCl, 0.5 mM MgCl<sub>2</sub>, 5 mM glucose, 0.1 % BSA, pH 7.4) to remove the excess Fluo-3/AM. The fluorescence of the loaded cells was analyzed

by flow cytometer (BD FACSCalibur, USA) at an emission wavelength of 530 nm and an excitation wavelength of 488 nm.

### Statistical analysis

Data were presented as means±standard deviation of three replicates. All statistical analyses were performed using the SPSS 17.0 software (SPSS, Chicago, IL, USA). The difference among the means of multiple groups was analyzed by one-way analysis of variance followed by LSD multiple comparison tests.  $P < 0.05$  was considered significant.

## Results

### Morphological effects of EET on HepG<sub>2</sub> cells

In previous report [7], we had observed that EET significantly induced DNA damages and nuclear chromatin condensation in HepG<sub>2</sub> cells by Hoechst 33258 staining. Morphological characterization of EET-induced apoptosis in HepG<sub>2</sub> cells was further examined with a double fluorescent dye (AO/EB) staining method. AO/EB staining consists in staining with EB which is only taken up by cells when the cellular membrane integrity is lost and stains the nuclei red and AO which permeates whole cells and makes the nuclei green. EB also dominates over AO [11].

Figure 1 demonstrated that distinct apoptotic morphological changes occurred in HepG<sub>2</sub> cells treated by EET for 24 h. In the control group, nuclei were homogeneously green without condensation (Fig. 1a). In the treatment group, the color of the nuclei was changed from green to red. The proportion of the bright orange or red cells increased obviously with increment of EET concentration, especially for the 200- $\mu\text{g}/\text{mL}$  treatment group; some chromatin condensation particles occurred in the nucleus (arrow showing).

### Apoptosis induced by EET and caspase inhibitor, alone or in combination

The apoptotic cell scatterplot could be composed of four subgroups: the lower right quadrant were early apoptotic cells (annexin V<sup>+</sup>/PI<sup>-</sup>), the upper right quadrant were the late apoptotic cells (annexin V<sup>+</sup>/PI<sup>+</sup>), the lower left quadrant were the normal cells, and the upper left quadrant were the damaged cells. The annexin V assay revealed the dose-dependent apoptotic effect of EET on HepG<sub>2</sub> cells. Negative control showed 91.8±3.2 % viability, 5.9±2.2 % in apoptosis (the proportion of early and late apoptotic cells), whereas after treated with 50  $\mu\text{g}/\text{mL}$  of EET, HepG<sub>2</sub> cells showed 84.6±4.1 % viability, 13.1±3.9 % in apoptosis. Both 100 and 200  $\mu\text{g}/\text{mL}$  of EET treatment groups showed significant increase in apoptosis

compared with control ( $P < 0.01$ ), apoptotic rates of them ranged from 23.7±5.3 % to 36.3±6.7 % (Fig. 2). To explore if apoptosis by EET could be blocked by inhibiting the caspase cascade, HepG<sub>2</sub> cells were treated with 100  $\mu\text{g}/\text{mL}$  EET for 24 h in the absence or presence of selective inhibitors (Z-LEHD-FMK for caspase-9, Z-IETD-FMK for caspase-8), respectively. Previously, we confirmed that these inhibitors themselves had no obvious impact on cell vitality because the apoptotic rates of HepG<sub>2</sub> cells treated with 15  $\mu\text{M}$  of Z-LEHD-FMK or Z-IETD-FMK alone were similar to that of control (Fig. 2). However, the co-treatment with 100  $\mu\text{g}/\text{mL}$  EET and Z-LEHD-FMK significantly inhibited the EET-induced apoptosis; the apoptotic rate decreased significantly to 16.9±2.9 % (compared with the 100  $\mu\text{g}/\text{mL}$  EET alone treatment,  $P < 0.05$ ). But the apoptotic rate remained almost unchanged in response to caspase-8 inhibitor. Thus, these results indicated that caspase-9 signal cascades participated in EET-induced apoptosis in HepG<sub>2</sub> cells, while caspase-8 did not.

### EET stimulated caspase-3 and caspase-9 activation, but not caspase-8

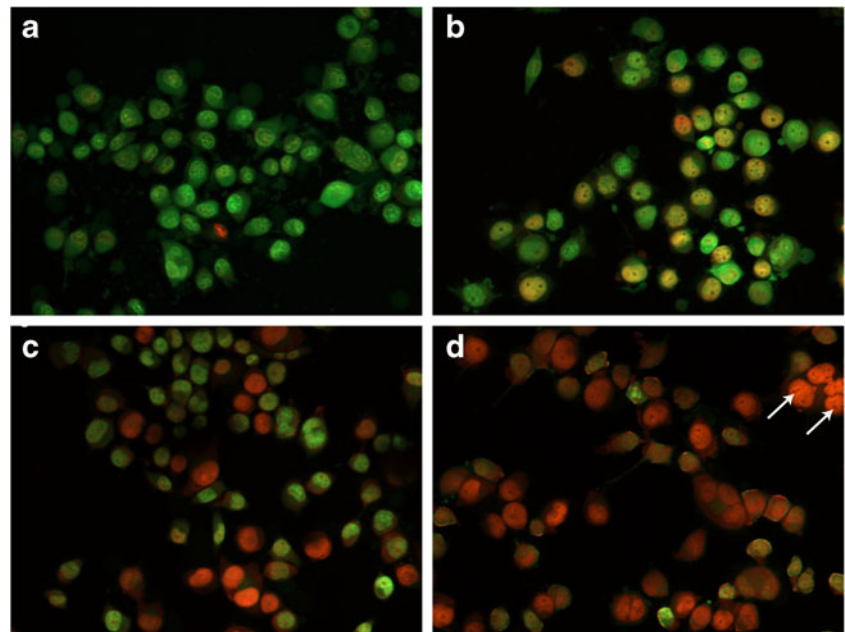
The activity of caspases was detected to investigate the role of death receptor and mitochondrial pathway in EET-induced apoptosis. The results presented in Fig. 3, indicating that EET induced the activation of caspase-3, and caspase-9, but not caspase-8, and the higher EET concentration was, the more obvious the enhancement effect was. Incubation with 200  $\mu\text{g}/\text{mL}$  EET revealed the strongest activation of caspase-3 or caspase-9, reaching 540.57±29 % and 280.34±19 %, respectively. The caspase-3 activity of EET-treated cells showed a sharp increase during 6 and 12 h, reached the maximum by 24 h, and then began an obvious decline. A similar rapid rise of caspase-9 activity occurred during 0 and 6 h, and then no further increase was observed. In contrast, there was no significant change in caspase-8 activity. Our investigations also revealed a sharp decline in the activities of all caspases occurred after 24-h incubation, specifically, exposed to 200  $\mu\text{g}/\text{mL}$  of EET. It was likely to be because the vitality of HepG<sub>2</sub> cells had mostly decayed, accompanied by the activation of cellular protein degradation. These results confirmed that activation of caspase-9 occurs during EET-induced apoptosis, which in turn activate the caspase-3 and lead cells to apoptosis, but caspase-8 activation might not be essential.

### EET regulated the expression of apoptosis-related protein in HepG<sub>2</sub> cells

Both the cleavage of PARP (the substrate of caspase-3) and activation of caspases are credible indicators of apoptosis. To further examine the effect of caspase-9 and caspase-3 on EET-



**Fig. 1** Micrographs of nuclei in HepG<sub>2</sub> cells after the treatment of EET detected by AO/EB staining. Cells were treated with 0.1 % DMSO (a) or 50  $\mu\text{g}/\text{mL}$  (b), 100  $\mu\text{g}/\text{mL}$  (c), and 200  $\mu\text{g}/\text{mL}$  (d) of EET for 24 h, respectively. The 58- $\mu\text{m}$  scale bar is applied to all figures



induced apoptosis, the protein expression level of PARP and caspases was then evaluated by western blotting. As can be seen in Fig. 4, the PARP protein degradation was significant after treatment with EET for 24 h; the expression levels of its active forms had gone up significantly and its precursor form were diminished with the increase of EET concentration. The exposure to EET also resulted in a significant downregulation of the precursor forms of caspase-9 and caspase-3, whereas cleaved caspase-9 was detectable in cells treated with high concentrations of EET. However, the precursor form of caspase-8 did not show any significant change with various EET concentrations, and its active form was not detected in EET-treated cells. Although there was a slight decline in the expression of procaspase-8 exposed to 200  $\mu\text{g}/\text{mL}$  of EET, the differences were not significant ( $P < 0.05$ ). The results further suggested that the sequential activation of caspase-9 and caspase-3 participated in EET-induced apoptosis.

#### **EET treatment resulted in mitochondrial membrane potential collapse and the release of cytochrome c**

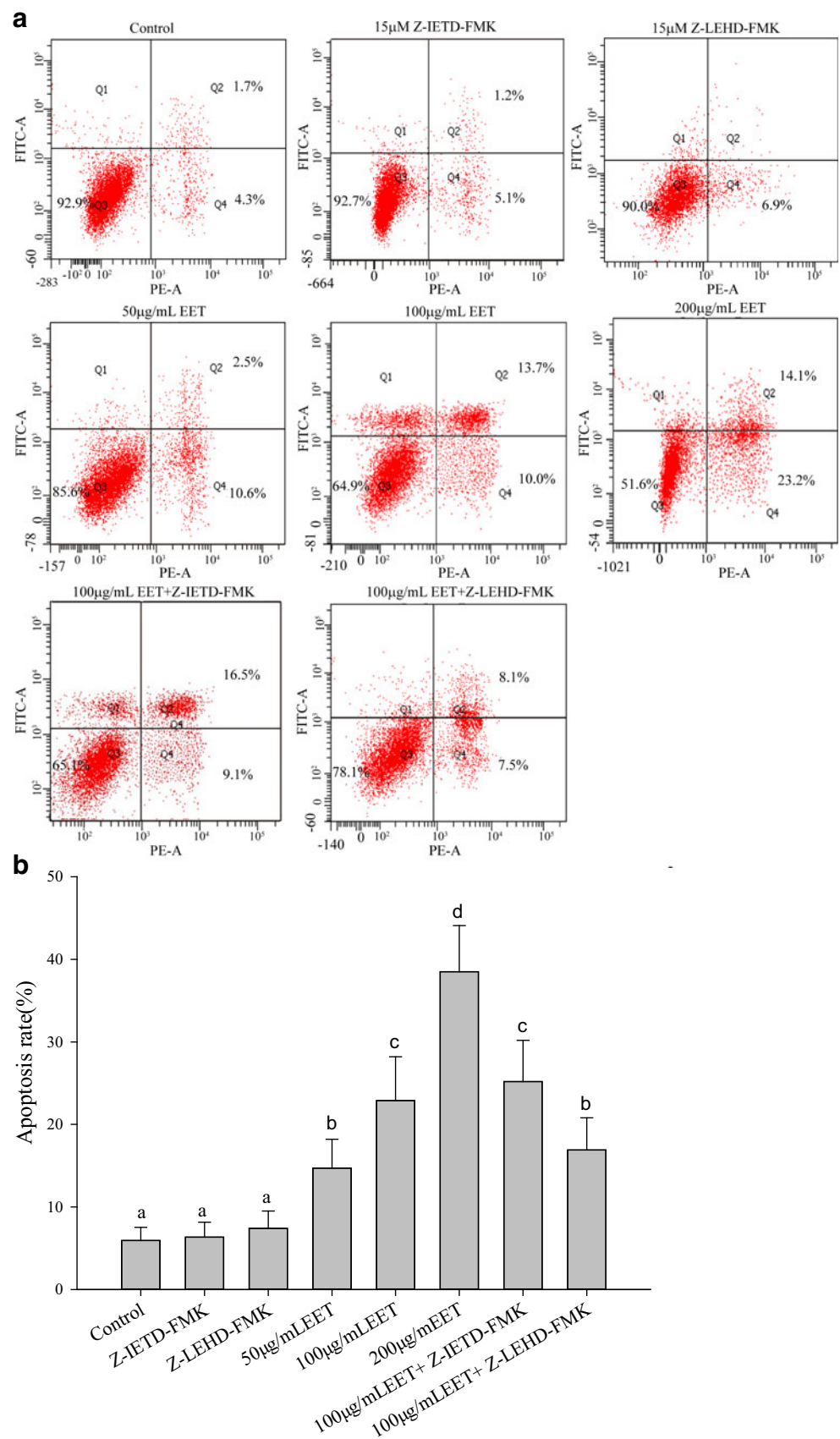
Mitochondrial dysfunction has been reported to play a vital role in intrinsic apoptosis processes, which is characterized by the collapse of transmembrane potential [12]. In view of the increase in levels of activated caspase-3 and caspase-9 that was observed in HepG<sub>2</sub> cells exposed to EET, we then evaluated whether treatment with EET induced a loss in mitochondria transmembrane potential ( $\Delta\psi\text{m}$ ) and the release of cytochrome c from mitochondria as proof of mitochondria-mediated apoptosis. The  $\Delta\psi\text{m}$  of HepG<sub>2</sub> cells was detected

by the fluorescent dye JC-1 using flow cytometer and inverted fluorescence microscope. JC-1 molecules accumulate in mitochondria as aggregate, thus rendering strong red fluorescence emission. However, in apoptotic cells, JC-1 molecules exist in the cytoplasm as monomers, which can be reflected by strong green and weak red fluorescence emission [13]. The ratio of green and red fluorescence indicates depolarization percentage of mitochondria. As shown in Fig. 5a, the analysis of inverted fluorescence microscope showed the obvious distinction between functional and collapsed membranes. EET significantly changed the fluorescence intensity from red to green in treated cells, which became obvious with the increasing concentration of EET. This suggested that treatment with EET significantly decreased the levels of  $\Delta\psi\text{m}$  in a concentration-dependent manner.

Fluorescence emission was further measured via flow cytometry. The results showed a remarkable increase in green fluorescence of JC-1 monomers in EET-treated cells (Fig. 5b). The increased ratio in green/red signal after EET treatment implied a loss in  $\Delta\psi\text{m}$ . The depolarization (red to green) was noticed in a concentration-dependent manner, and the maximum depolarization was observed at 200  $\mu\text{g}/\text{mL}$ . The ratio of green/red fluorescence signal increased to  $6.06 \pm 1.7$ ,  $16.81 \pm 2.8$ ,  $64.29 \pm 7.5$ , and  $288.77 \pm 18.5$  % with EET at the concentration of 0, 50, 100, and 200  $\mu\text{g}/\text{mL}$ , respectively ( $P < 0.05$ ).

In addition, mitochondrial dysfunction often induces the pro-apoptotic proteins such as Cyt-c releasing from the mitochondria to the cytosol and subsequently causing a caspase-dependent apoptosis [14]. The release of cytochrome c from

**Fig. 2** Apoptosis induced by EET (0, 50, 100, and 200  $\mu\text{g}/\text{mL}$ ) and caspase inhibitor, alone or in combination. Representative flow cytometric graphs of three independent experiments are shown. *Bar graphs* show the apoptosis rate of all treatments. *Different English letters on the column* indicate a significant difference, compared with each other by LSD multiple comparison test ( $P < 0.05$ ), respectively. Values are presented as means  $\pm$  SD of three independent experiments



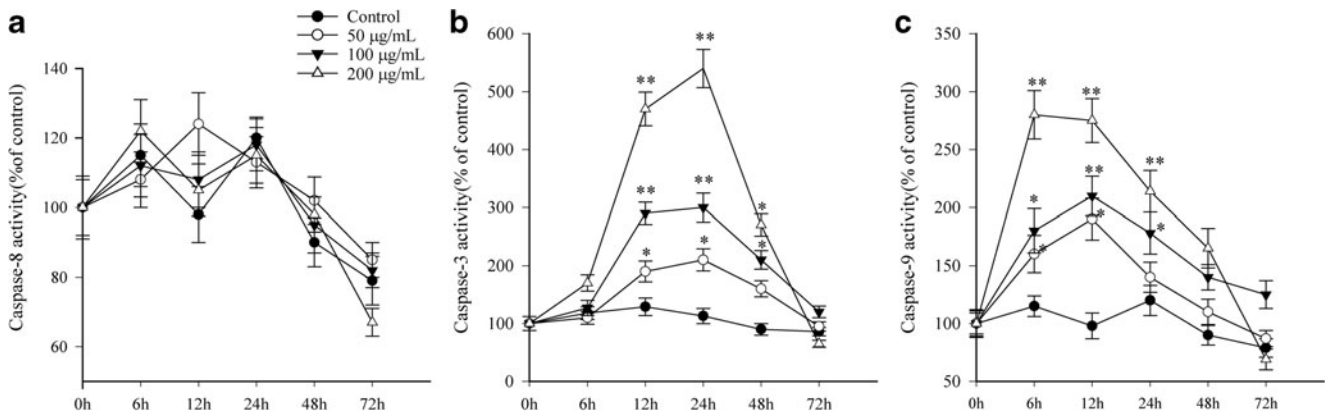


**Fig. 3** Effects of EET (0, 50, 100, and 200 µg/mL) on the activities of caspase-8 (a), caspases-3 (b), and caspase-9 (c) for indicated time intervals. The detection of caspases activities were performed using ELISA.

\* $P < 0.05$  and \*\* $P < 0.01$ , respectively, versus control using ANOVA test. Values are presented as means  $\pm$  SD of three independent experiments

mitochondria to cytosolic was investigated separately in mitochondria and cytosolic fractions of EET-treated cells. As seen from Fig. 6, treatment of cells with EET for 24 h induced a substantial cytochrome c release; the Cyt-c levels of cytosolic fractions increased with exposure to increasing concentrations of EET, while that of mitochondria fractions decreased. When treated with 100 or 200 µg/mL of EET, the amount of Cyt-c significantly decreased in mitochondria while increased in cytosol, compared with control ( $P < 0.05$ ).

Therefore, our findings suggested that EET induced the dysfunction of  $\Delta\psi_m$ , leading to the release of cytochrome c from mitochondria to cytosolic, which aimed to activate caspase-dependent apoptosis.

### EET treatment elevated intracellular $Ca^{2+}$ levels

Mitochondria is an intracellular calcium pool; the change of mitochondrial membrane potential would result in the calcium influx or intracellular calcium release, and on the other hand, the calcium influx or intracellular calcium release is also a direct reason for the decrease of mitochondrial membrane potential.

Fluo-3 was used as the intracellular free  $Ca^{2+}$  indicator, and cells were loaded with its ester form, Fluo-3/AM. To assess the influence of EET on cytosolic  $Ca^{2+}$ , we examined in intracellular free  $Ca^{2+}$  levels in response to treatment with different concentrations of EET. As

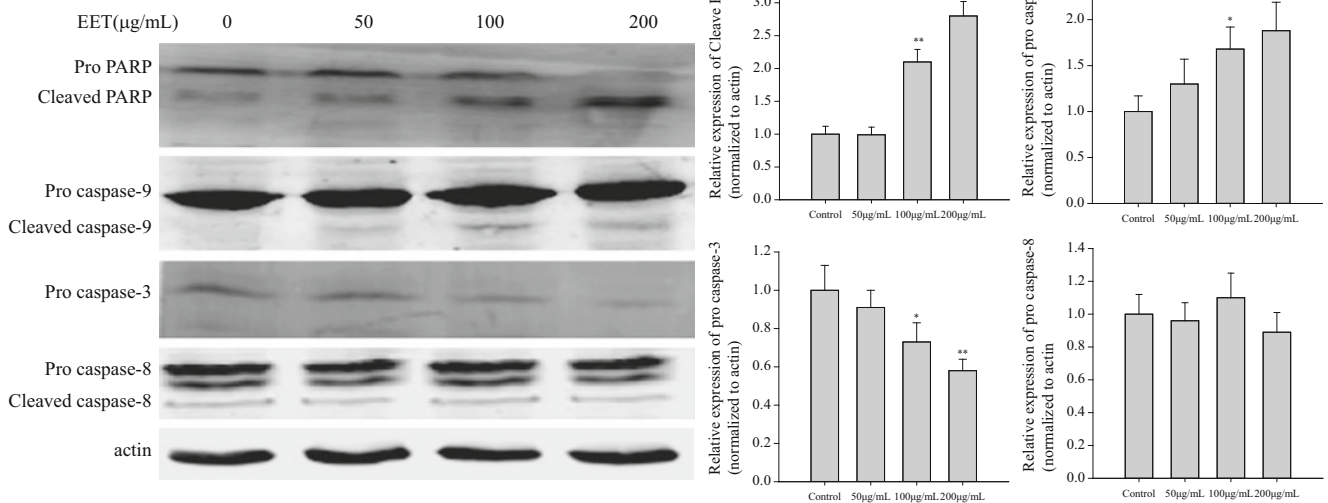
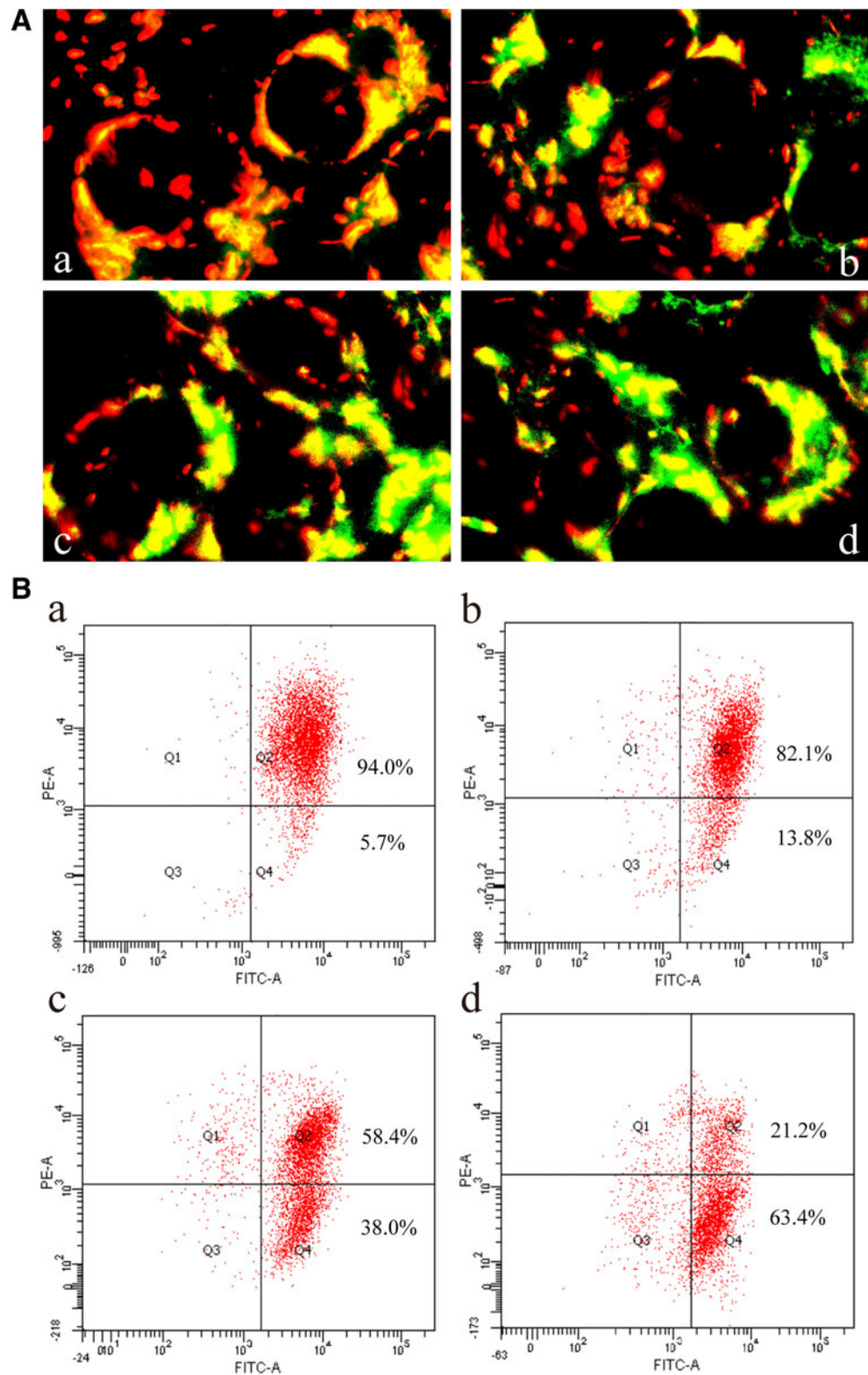


**Fig. 4** Effects of EET on the protein expression of caspases and the cleavage of PARP in HepG<sub>2</sub> cells. HepG<sub>2</sub> cells were treated with 0, 50, 100, and 200 µg/mL EET, respectively. Representative blots of three

independent experiments are shown. \* $P < 0.05$  and \*\* $P < 0.01$ , respectively, versus control using ANOVA test

**Fig. 5** EET alters the mitochondria transmembrane potential in HepG<sub>2</sub> cells. **(A)** Fluorescence photomicrograph of 264 change in  $\Delta\psi_m$  after EET treatment. **(B)**  $\Delta\psi_m$  is expressed as JC-1 fluorescence units in terms of green fluorescence to red fluorescence ratio using flow cytometer. Cells were treated with 0.1 % DMSO **(a)** or 50  $\mu\text{g}/\text{mL}$  **(b)**, 100  $\mu\text{g}/\text{mL}$  **(c)**, and 200  $\mu\text{g}/\text{mL}$  **(d)** of EET for 24 h, respectively ( $\times 1000$  magnification). Representative results of three independent experiments are shown



shown in Fig. 7, EET increased the Fluo-3 fluorescence intensity in HepG<sub>2</sub> cells in a concentration-dependent manner. Fluo-3 fluorescence intensity increased from  $17.5 \pm 4.6$  % (control) to  $58.4 \pm 4.3$  % (50  $\mu\text{g}/\text{mL}$  EET-

treated),  $80.7 \pm 6.6$  % (100  $\mu\text{g}/\text{mL}$  EET-treated), and  $92.1 \pm 3.9$  % (200  $\mu\text{g}/\text{mL}$  EET-treated), respectively ( $n=3$ ,  $P<0.01$ ). It indicated that EET strongly enhanced the intracellular  $\text{Ca}^{2+}$  levels in HepG<sub>2</sub> cells.



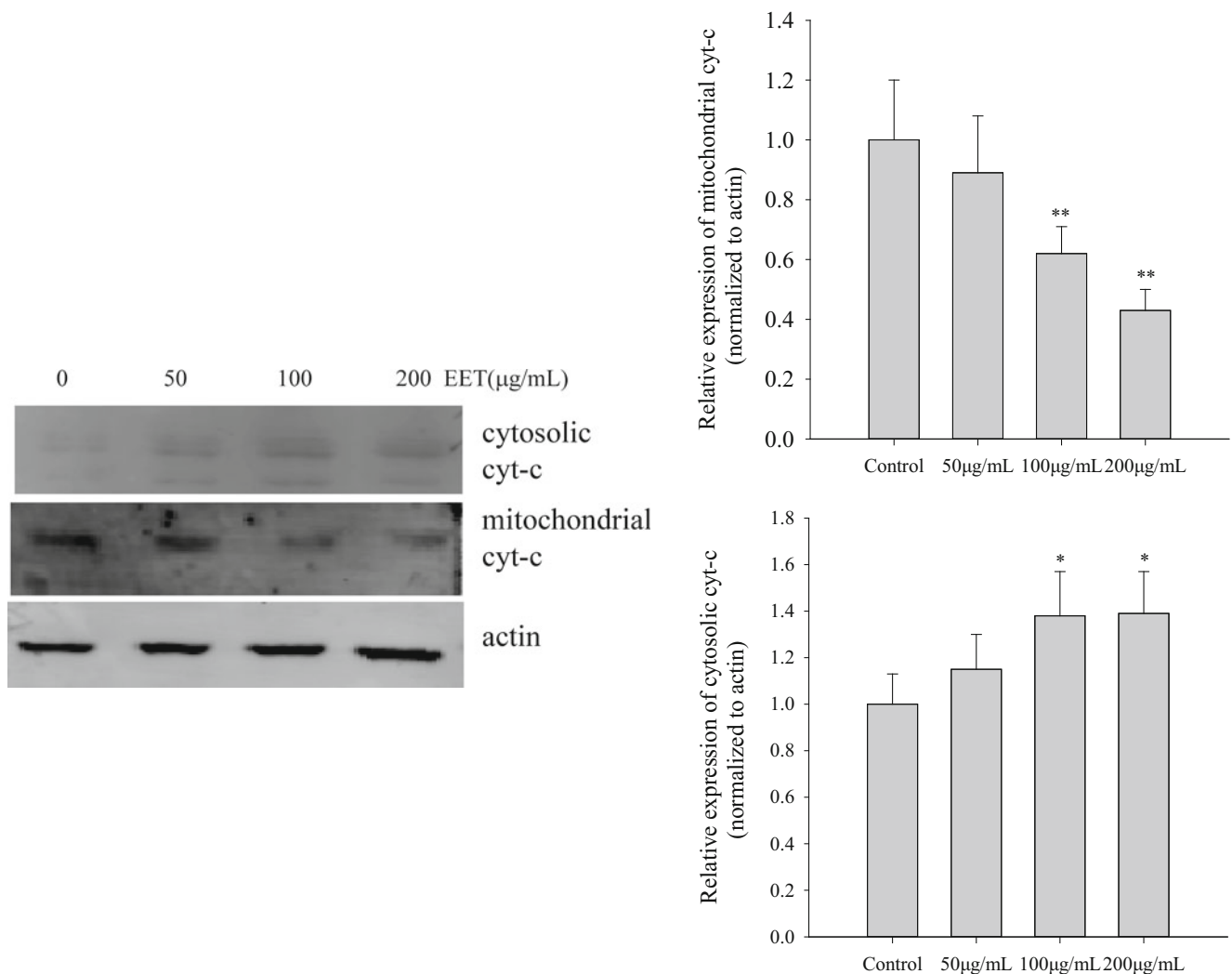


**Fig. 6** EET (50, 100, and 200 µg/mL) induced the release of cytochrome c from mitochondria to cytosolic. Representative blots of three independent experiments are shown. *Bar graphs* show the relative

expression level of the blots. \* $P < 0.05$  and \*\* $P < 0.01$ , respectively, versus control using ANOVA test. Values are presented as means  $\pm$  SD of three independent experiments

## Discussion

Apoptosis, also known as programmed cell death, plays a crucial role in preventing normal cells from turning into cancerous ones. It involved a cascade of biochemical reactions leading to membrane blebbing, chromatin condensation, and DNA fragmentation of the nucleus [15]. Many researches had been focused on natural biological active compound for examining their ability to induce or enhance apoptosis in cancer cells. Recently, the antitumor activity of EET has been reported in various cancer types [5, 6]. Our previous studies [7] indicated that the morphology of EET-treated HepG<sub>2</sub> cells showed evidence of apoptosis including membrane blebbing, cellular shrinkage, chromatin condensation, and nucleic fragmentation. The results of AO/EB double fluorescence staining in the present study also demonstrated that distinct apoptotic morphological changes occurred in HepG<sub>2</sub> cells treated by

EET. However, the molecular mechanisms underlying EET-induced apoptosis have not been well illuminated. The present study was focused on characterizing the EET-induced apoptotic signaling pathways in HepG<sub>2</sub> cells, which was an important step in this drug development process.

Apoptosis is strictly regulated through a diverse range of cell signals; overall, they can be divided into two major pathways: the death receptor-induced extrinsic pathway and the mitochondria-mediated intrinsic pathway [16]. The death receptor extrinsic pathway activated the death receptor (Fas and tumor necrosis factor) on cell surface, then promoted caspase-8 activation, and finally led to the activation of caspase-3 (a principle effector caspase). The mitochondrial intrinsic pathway is often triggered by a disruption of mitochondrial membrane potential (MMP) and then the release of cytochrome c from mitochondria to cytosol, activation of caspase-9 (an initiator caspase of

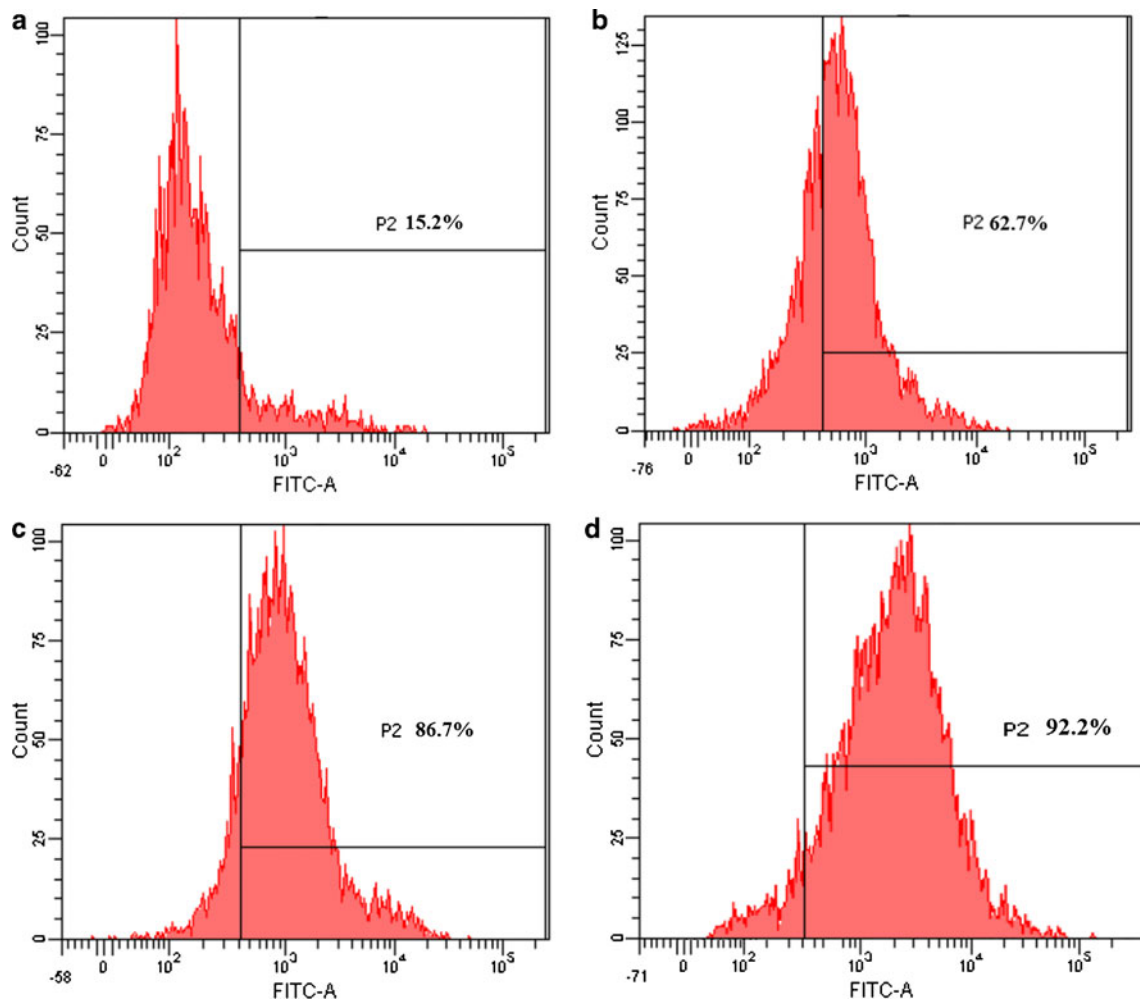


**Fig. 7** EET induced the elevation of cytosolic  $\text{Ca}^{2+}$  level. Representative flow cytometric graphs of three independent experiments are shown. Cells were treated with 0.1 %DMSO (a) or 50  $\mu\text{g}/\text{mL}$  (b), 100  $\mu\text{g}/\text{mL}$  (c), and 200  $\mu\text{g}/\text{mL}$  (d) of EET for 24 h, respectively

the intrinsic pathway), which ultimately cleave procaspase-3 to form active caspase-3. Disruption of MMP and the subsequent release of apoptogenic molecules such as  $\text{Ca}^{2+}$ , Cytc, and some caspases are considered as an early event that trigger the intrinsic apoptotic pathway [17]. Based on the results of flow cytometer and inverted fluorescence microscope in the present study, we clearly demonstrated that HepG<sub>2</sub> cells treated with EET exhibited a collapse of MMP, suggesting that mitochondria might play a crucial role in EET-induced apoptosis.

$\text{Ca}^{2+}$  is a prominent modulator of mitochondrial permeability transition (PT). The PT has been regarded as a mechanism of apoptosis after selected stimuli.  $\text{Ca}^{2+}$  signaling can be modulated and synchronized by mitochondria. Stimuli that generate inositol 1,4,5-tris-phosphate (IP<sub>3</sub>) cause release of  $\text{Ca}^{2+}$  from calcium pool in endoplasmic reticulum (ER) [9]. Members of the Bcl<sub>2</sub> family are also involved in  $\text{Ca}^{2+}$  signaling pathway, such as Bax and Bcl<sub>2</sub>. The overexpression of proapoptotic Bax could result in a release of ER  $\text{Ca}^{2+}$ , with a

subsequent increase in mitochondria  $\text{Ca}^{2+}$ , and facilitate the release of Cytc by promoting the opening of the mitochondrial permeability transition pore [18]. Consequently, caspase-9 and caspase-3 were activated. The overexpression of antiapoptotic Bcl<sub>2</sub> has an opposite effect, compared with Bax. Our previous study [7] showed that a decrease expression of Bcl<sub>2</sub> and an increase expression of Bax were observed in HepG<sub>2</sub> cells after treatment with EET. To further demonstrate the induction of apoptosis by EET, the mitochondrial membrane depolarization and the cytosolic  $\text{Ca}^{2+}$  level were examined in the present study, using JC-1 a carbocyanine fluorescence dye and Fluo-3 an intracellular free  $\text{Ca}^{2+}$  indicator, respectively. The results showed that treatment of HepG<sub>2</sub> cells with EET caused a collapse of MMP and an increase of the intracellular  $\text{Ca}^{2+}$  in a concentration-dependent manner, which might result from the changes in Bax and Bcl<sub>2</sub> proteins expression. The mitochondrial  $\text{Ca}^{2+}$  accumulation contributed to the activation of endonucleases that degrade DNA and then led to cell apoptosis [19]. Our previous study [7] had shown

that obvious DNA ladders were observed in 100 or 200  $\mu\text{g}/\text{mL}$  EET-treated HepG<sub>2</sub> cells, which was in consistent with the present report that showed EET induced an intracellular Ca<sup>2+</sup> rise.

Caspases play pivotal roles in the activation of apoptotic signal transmission and completion of apoptosis. They are divided into initiators (e.g., caspase-8, caspase-9, caspase-12) and executors (e.g., caspase-3, caspase-6, caspase-7), and they are synthesized as relatively inactive zymogens, which become activated upon cleavage. Consequently, this cleavage contributes to the morphological and biochemical changes that constitute the process of apoptosis. Determination of caspases activity was also carried out in this study. Elevation of caspase-9 and caspase-3 by EET was initiated after 6 or 12 h of EET exposure and maintained to 24 h, whereas there was no significant change in caspase-8 activity. Consistent with these results, the results of western blotting demonstrated that treatment with EET activated caspase-3 and caspase-9, induced the release of Cyt c from mitochondria into cytosol, as well as promoted PRAP degradation. It was observed that caspase-9 was activated in a dose-dependent manner and a subunit occurred, which subsequently activated the downstream effector caspase-3, accompanied by the reduction of the amounts of the procaspase-3. Activated caspase-3 is responsible for the proteolytic degradation of poly ADP-ribose polymerase, which occurs at apoptosis onset [20]. PARP is a nuclear enzyme that responds to DNA damage and facilitates DNA repair and promotes cell survival. When apoptosis occurs, it is cleaved to an 85-kD fragment by caspase-3 [21]. In this study, the EET-induced cleavage of PARP was also observed clearly after EET treatment, suggesting that PARP was involved in EET-induced cell apoptosis. The results of western blotting also showed that procaspase-8 level remained almost unchanged after EET treatment.

Furthermore, the roles of caspases in EET-induced apoptosis were confirmed by using the selective caspase inhibitors. Flow cytometry data on AnnexinV-PI double staining showed that EET increased the number of early and late apoptotic cells in a dose-dependent manner compared with untreated cells. The EET-induced apoptosis was significantly blocked after caspase-9 inhibitor (Z-LEHD-FMK) pretreatment, whereas the apoptotic rate remained almost unchanged in response to caspase-8 inhibitor (Z-IETD-FMK). Therefore, the caspase-9 played an upstream regulatory role in the interaction of the mitochondria and downstream caspases; however, caspase-8 and the death receptor-induced extrinsic pathway did not seem to be involved in EET-induced apoptosis.

In summary, EET induced a disruption of MMP, elevation of intracellular Ca<sup>2+</sup>, release of cytochrome c, activation of caspase-9, and cleavage of PARP. All these typically signal within the intrinsic pathway acting on downstream effector caspase-3. Together, the caspase-

dependent intrinsic pathway virtually contributed to EET-induced apoptosis of HepG<sub>2</sub> cells, whereas the death receptor/caspase-8-mediated signaling route seemed less important.

Our study showed that EET could be considered as a new preventive or therapeutic agent against HepG<sub>2</sub> cells; it might contain bioactive compounds capable of inducing apoptosis. Further study is needed to identify the anticancer compounds in EET, and the in vivo studies on the effects of EET are also necessary to determine its potential for clinical use.

**Acknowledgments** This work was supported by the traditional Chinese medical science technology research projects of Zhejiang Province (Grant No. 2013ZA119), the public welfare technology research projects of Zhejiang Province (Grant No. 2013C32103), and the agricultural research projects of Ningbo City (Grant No. 2014C10031).

**Conflicts of interest** None

**Authors' contributions** Xin Peng contributed for cell culture, western blotting, and statistical analysis and wrote the manuscript. Yuan-yuan Zhang contributed for the detection of cell apoptosis ratio. Jin Wang contributed for the detection of the apoptotic morphological changes. Qingyong Ji was responsible for the preparation of EET.

## References

- Zhao JL, Zhao J, Jiao HJ. Synergistic growth-suppressive effects of quercetin and cisplatin on HepG<sub>2</sub> human hepatocellular carcinoma cells. *Appl Biochem Biotechnol*. 2014;172:784–91.
- Fulda S, Debatin KM. Extrinsic versus intrinsic apoptosis pathways in anticancer chemotherapy. *Oncogene*. 2006;25:4798–811.
- Fei HR, Chen HL, Xiao T, et al. Caudatin induces cell cycle arrest and caspase-dependent apoptosis in HepG<sub>2</sub> cell. *Mol Biol Rep*. 2012;39:131–8.
- Xu CJ, Ding GQ, Fu JY, et al. Immunoregulatory effects of ethylacetate fraction of extracts from *Tetragonia hemsleyanum* Diels et Gilg on immune functions of ICR mice. *Biomed Environ Sci*. 2008;21:325–31.
- He FG. Research progress in anticancer effect of *Tetragonia hemsleyanum* Diels et Gilg and its mechanism. *J Oncol*. 2010;16:75–7 (in Chinese).
- Yuming Y, Yili W, Yeling T, et al. Comparative study on anti-tumor effects of different processed *Tetragonia hemsleyanum* Diels et Gilg on Lewis lung cancer and H22 liver cancer in mice. *Chin Arch Tradit Chin Med*. 2013;31:2674–6 (in Chinese).
- Peng X, Zhuang DD, Guo QS. Induction of S phase arrest and apoptosis by ethylacetate extract from *Tetragonia hemsleyanum* in human hepatoma HepG<sub>2</sub> cells. *Tumor Biol*. 2015. doi:10.1007/s13277-014-2869-x.
- Nagata S. Apoptosis by death factor. *Cell*. 1997;88:355–65.
- Li P, Zhao QL, Wu LH, et al. Isofraxidin, a potent reactive oxygen species (ROS) scavenger, protects human leukemia cells from radiation-induced apoptosis via ROS/mitochondria pathway in p53-independent manner. *Apoptosis*. 2014;19:1043–53.
- Wen XX, Jian Z, Dan Z, et al. Denatonium inhibits growth and induces apoptosis of airway epithelial cells through mitochondrial signaling pathways. *Respir Res*. 2015;16:13–22.
- Byczkowska A, Kunikowska A, Kaźmierczak A. Determination of ACC-induced cell-programmed death in roots of *Vicia faba* ssp.

- minor seedlings by acridine orange and ethidium bromide staining. *Protoplasma*. 2013;250:121–8.
12. Kim MS, Bak Y, Park YS, et al. Wogonin induces apoptosis by suppressing E6 and E7 expressions and activating intrinsic signaling pathways in HPV-16 cervical cancer cells. *Cell Biol Toxicol*. 2013;29:259–72.
  13. Looi CY, Moharram B, Paydar M, et al. Induction of apoptosis in melanoma A375 cells by a chloroform fraction of *Centratherum anthelminticum* (L.) seeds involves NF-kappaB, p53 and Bcl-2-controlled mitochondrial signaling pathways. *BMC Complem Altern Med*. 2013;13:166–79.
  14. Zhang Y, Zhao L, Li X, et al. V8, a newly synthetic flavonoid, induces apoptosis through ROS mediated ER stress pathway in hepatocellular carcinoma. *Arch Toxicol*. 2014;88:97–107.
  15. Banfalvi G. Apoptotic agents inducing genotoxicity-specific chromatin changes. *Apoptosis*. 2014;19:1301–16.
  16. Frenzel A, Grespi F, Chmielewski W, et al. Bcl<sub>2</sub> family proteins in carcinogenesis and the treatment of cancer. *Apoptosis*. 2009;14:584–96.
  17. Sun SL, Guo L, Ren YC, et al. Anti-apoptosis effect of polysaccharide isolated from the seeds of *Cuscuta chinensis* Lam on cardiomyocytes in aging rats. *Mol Biol Rep*. 2014;41:6117–24.
  18. Yan F, Liu Y, Wang WB. Matrine inhibited the growth of rat osteosarcoma UMR-108 cells by inducing apoptosis in a mitochondrial-caspase-dependent pathway. *Tumor Biol*. 2013;34:2135–40.
  19. Li JX, Shen YQ, Cai BZ, et al. Arsenic trioxide induces the apoptosis in vascular smooth muscle cells via increasing intracellular calcium and ROS formation. *Mol Biol Rep*. 2010;37:1569–76.
  20. Lazebnik YA, Kaufmann SH, Desnoyers S, et al. Cleavage of poly (ADP-ribose) polymerase by a proteinase with properties like ICE. *Nature*. 1994;371:346–7.
  21. Wang XB, Gao HY, Hou BL, et al. Nanoparticle realgar powders induce apoptosis in U937 cells through caspase MAPK and mitochondrial pathways. *Arch Pharm Res*. 2007;30:653–8.